An orientation-independent estimation of the earthquake-induced sliding displacement of slopes

Jian Song & Yufeng Gao
Key Laboratory of Ministry of Education for Geomechanics and Embankment Engineering, Hohai University, Nanjing 210098, China

Adrian Rodriguez-Marek
Department of Civil and Environmental Engineering, Virginia Tech, Blacksburg, VA 24060, USA

ABSTRACT

Empirical predictive relationships of sliding displacement are commonly used in the seismic hazard assessment of slopes. However, the current relationships were developed by computing the displacements from a set of selected ground motions, and then correlating these displacements with optimal ground motion parameters of the ground motion time histories. The ground motion parameters associated with the particular time histories are different from those for directionally-dependent parameters that are generally used in the ground motion prediction equations. In this paper, the rigid sliding displacements of slopes are computed for a set of ground motion records by rotating the horizontal components through all angles. It is found that the sliding displacement can be dependent on the orientation of ground motions. The distribution of sliding displacements in various orientations, and the orientations in which the maximum sliding displacements occur are examined. The predictive relationships developed using the computed sliding displacement at various orientations are compared. Finally, an orientation-independent estimation of the earthquake-induced sliding displacement of slopes is provided to connect to the directionally-dependent shaking parameters in the latest ground motion prediction equations.

1 INTRODUCTION

The sliding displacement due to earthquake shaking is commonly used to assess the seismic performance of slopes. The rigid sliding block model (Newmark 1965) has become the most prevalent method to evaluate the stability of slopes during earthquakes. Based on the rigid sliding block model, empirical predictive relationships of the displacement are widely used to estimate the landslide hazard. These relationships have been developed as a function of the yield acceleration of slope (k_y) and optimal ground motion intensity measures (IMs) (e.g., Makdisi and Seed 1978; Ambraseys and Menu 1988; Jibson 2007; Bray and Travasarou 2007; Saygili and Rathje 2008; Rathje and Saygili 2009; Rathje and Antonakos 2011; Hsieh and Lee 2011; Lee and Green 2015; Song and Rodriguez-Marek 2015; Song et al. 2016). These empirical relationships significantly simplify the assessment procedure for earthquake-induced landslides, particularly at a reginal scale.

The estimate of seismic displacement hazard based on the empirical relationships of displacement requires the prediction of ground motion IMs, which is generally through the ground motion prediction equations (GMPEs). Due to that earthquake ground motions produce two orthogonal ground shakings in the horizontal plane, and the ground motions can vary in different horizontal directions, the GMPEs often provide the ground motion intensity for a single definition of bidirectional ground motion. For example, the NGA-West2 research program has produced models for predicting the median IMs of a ground motion when rotated over all horizontal orientations (*RotD*50 value, Boore 2010). These values for different IMs may also occur in different orientations, and thus they are not from the same ground motion time history and do not represent any particular ground motion component. However, current predictive relationships of sliding displacement were developed by computing the displacement from a set of as-recorded components of ground motions, and then correlating these displacements with optimal ground motion parameters of the ground motion time histories. The displacement predicted from the relationship is for the ground motion IMs of a specific ground motion time history. These IMs are different from those predicted from GMPEs. Therefore, the use of ground motion IMs is not consistent throughout the assessment process of seismic performance of earth slopes. In addition, a question to ask is what does the displacement predicted from the traditional empirical relationships represents.

This study aims at comparing the predictive relationships developed using the computed sliding displacement at various orientations and providing a simplified method to include the effects of ground motion directionality on the assessment of earthquake-induced landslide hazard. Rigid sliding displacements are computed for a subset ground motion records from the NGA-West2 database by rotating the horizontal components of each record through all angles. The distribution of sliding displacement in all orientations and the orientations of maximum sliding displacement are examined. Empirical relationships are provided to predict

the maximum and the median sliding displacement through all orientation based on directionally-dependent ground motion IMs. These ground motion IMs are consistent with those used in the latest ground motion prediction equations in NGA-West2 program of PEER. The predicted median sliding displacement and the variation of standard deviation of these relationships are compared.

2 GROUND MOTION DATABASE

The subset of the Pacific Earthquake Engineering Research Center's PEER-NGA-West2 strong motion database (Ancheta et al. 2012) is used to compute the Newmark displacement. Ground motions with the moment magnitude $5.5 \le M_w \le 7.9$ and with closest distance to the rupture fault $R_{rup} \le 100$ km were selected to focus on the range of magnitudes and distances that will generally control the landslide hazard in high seismicity regions. Ground motions recorded at soft soil sites were removed from the database, and only horizontal recordings from free-field conditions are used in the analysis, resulting in a total of 2496 pairs of ground motions of two horizontal directions from 102 worldwide earthquake events.

Rigid sliding block displacements were computed by Newmark's sliding block method for k_y values of 0.02, 0.05, 0.1, 0.15, 0.2, 0.3 g. In traditional studies on the development of predictive relationships of the sliding displacement (e.g., Saygili and Rathje 2008; Hsieh and Lee 2011; Lee and Green 2015), two horizontal recordings at the same station are treated as independent records. In this study, the ground motions were rotated through 0-180° based on the two recorded orthogonal components. Then the rigid sliding displacements were computed for all the horizontal components with various rotation angles for each ground motion record. The displacements are computed for both positive and negative directions for each record, and the maximum value is taken for analyses.

3 DISTRIBUTION OF RIGID SLIDING DISPLACEMENT IN DIFFERENT ORIENTATIONS

The maximum and the minimum sliding displacements through all orientations for each ground motion record are compared, and the normalized difference in the sliding displacement is calculated using:

$$Normalized\ difference = (D_{\max} - D_{\min}) / D_{\max} \quad [1]$$

Figure 1 shows the distribution of the normalized difference of sliding displacement for rigid blocks with different k_y values. Observe that most normalized differences are larger than 0.5 for all k_y values, which indicates that the maximum displacement is significantly larger than the minimum displacement. The differences are much more prominent as the yield acceleration of the block k_y increases. The number of the normalized difference that equals to one becomes dominant for larger k_y values. This is the result of the increasing number of cases where the minimum displacement is zero as the strength of slope increases. These observations imply that the sliding displacement of slopes can be significantly varied through different orientations.

The orientation in which the maximum sliding displacement occurs is also examined, and the distribution is shown in Fig. 2. The maximum displacement could be occurred in all rotation angles from the fault strike, and there is no tendency towards a particular orientation. Previous studies on the ground motion directionality concluded that the maximum orientation of a spectral acceleration is more likely to be closer to the strike-normal direction at periods greater than about 1 s when the closest distance is within 5 km of the fault (e.g., Howard et al. 2005; Watson-Lamprey and Boore 2007; Huang et al. 2008, 2009; Shahi and Baker 2014). In view of this, the distribution of the orientation of the maximum sliding displacement direction relative to the fault strike is separated for ground motions with $R_{rup} < 5$ km and $R_{rup} > 5$ km, respectively, and the results are illustrated in Fig. 3. A pronounced polarity of the sliding displacement to the fault-normal direction is observed for ground motions with $R_{rup} < 5$ km, while the maximum direction orientation is almost uniformly distributed for ground motions with $R_{rup} > 5$ km. This is consistent with the observations in ground motion directionality. The previous observations have indicated that the characteristics of ground motion directionality could lead to orientation-dependent sliding displacements of slopes. The distribution of orientation of the maximum sliding displacement direction is useful to determine the occurrence orientation of landslides during an earthquake.

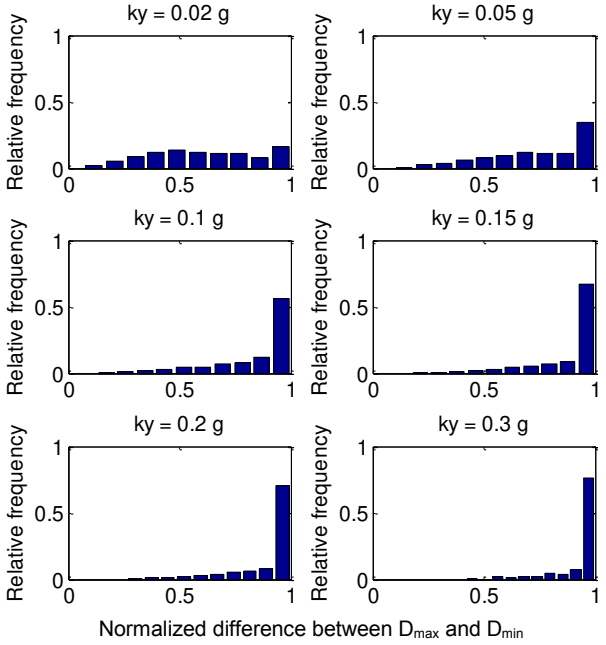

Figure 1. Histogram of the normalized difference between the maximum sliding displacement (D_{max}) and minimum sliding displacement (D_{min}) for different k_y values.

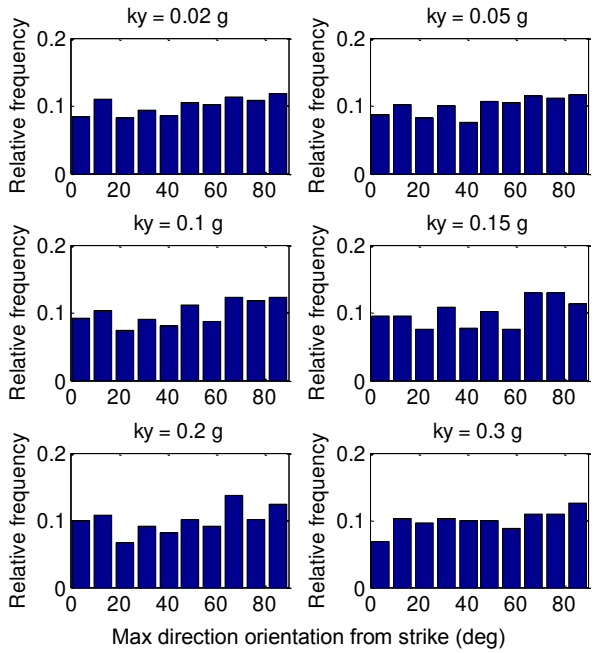

Figure 2. Histogram of the orientation of the maximum sliding displacement direction relative to the fault strike for different k_y values.

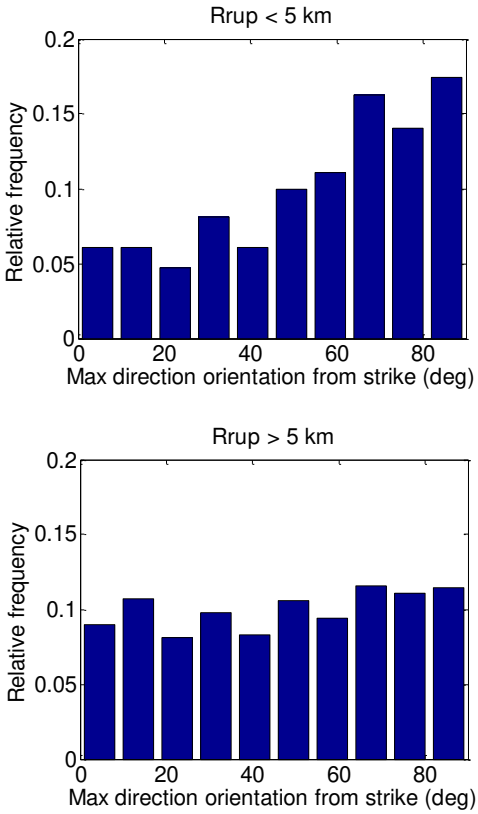

Figure 3. Histogram of the orientation of the maximum sliding displacement direction relative to the fault strike for ground motions with R_{rup} < 5 km and R_{rup} > 5 km.

4 PREDICTIVE RELATIONSHIPS BASED ON SLIDING DISPLACEMENTS AND GROUD MOTION PARAMETERS AT VARIOUS ORIENTATIONS

Due to that both ground motion IMs and sliding displacement of slopes can be significantly varied through different orientations, a question to ask is whether there is a distinction among the predictive relationships developed using the sliding displacement of slopes at various orientations. The empirical relationships of sliding displacements for the ground motion shaking at different orientations are compared. This is given as:

$$[\ln D]_{Rot(i)} = f[k_y, \mathrm{IMs}_{Rot(i)}] \quad [2]$$

where $[\ln D]_{Rot(i)}$ is the sliding displacement under the ground motion of the *i* orientation from the fault strike and $\mathrm{IMs}_{Rot(i)}$ is the value in the *i* orientation of the ground motion parameters used in the function. The functional forms of the predictive relationships developed by Saygili and Rathje (2008) and Rathje and Saygili (2009) are selected to make regression, including a scalar (PGA, M) model (Eq. 3) and a vector (PGA, PGV) model (Eq. 4), referred to as RS09(PGA, M) and SR08(PGA, PGV) forms, respectively:

$$\ln D = a_1 + a_2(ky/PGA) + a_3(ky/PGA)^2 + a_4(ky/PGA)^3 + a_5(ky/PGA)^4 + a_6\ln(PGA) + a_7(M-6) \quad [3]$$

$$\ln D = a_1 + a_2(ky/PGA) + a_3(ky/PGA)^2 + a_4(ky/PGA)^3 + a_5(ky/PGA)^4 + a_6\ln(PGA) + a_7\ln(PGV) \quad [4]$$

The regression analyses are made by using the least squares method. The coefficients for the two predictive relationships using different displacement data are given in Tables 1 and 2.

The median displacements predicted from the relationships developed by the ground motion IMs and the computed sliding displacements at various orientations are shown in Fig. 4. The sliding displacement is for a specific scenario: M_w = 7, R_{jb} = 6 km, rock site conditions (V_{s30} = 760 m/s), and a strike-slip faulting. The corresponding values of PGA and PGV used to predict the displacement are 0.33 g and 30 cm/s, which are the median values predicted from the Boore et al. (2014) ground motion prediction relationship. Additionally, In view of the prevalent use of the displacement data for two recorded ground motion components in developing the empirical predictive relationship of sliding displacement, the relationship is also developed by using computed displacements and the corresponding ground motion IMs for the two recorded components. The results indicate that the median sliding displacement is almost identical from different predictive relationships. The variation of standard deviation with k_y/PGA for different predictive

relationships is shown in Fig. 5. The distribution of standard deviation is generally similar for different relationships, except for the cases for 100° and 120° from the fault strike at large k_y/PGA values. The observations in Figs. 4 and 5 indicate that the predictive relationship is independent of the orientations in which the displacement data and the ground motion intensity are used in the development, although both ground motion IMs and sliding displacement of slopes can be orientation-dependent.

Table 1. The coefficients for the scalar (PGA, M) model developed based on different displacement data.

Sliding displacement used in the regression	a_1	a_2	a_3	a_4	a_5	a_6	a_7
0° from the strike	4.46	-4.35	-28.72	64.18	-43.22	0.66	0.87
20° from the strike	4.37	-1.54	-42.07	87.11	-55.84	0.68	0.83
40° from the strike	4.52	-2.58	-36.67	77.52	-50.44	0.71	0.82
60° from the strike	4.63	-3.10	-34.32	73.35	-48.04	0.73	0.81
80° from the strike	4.70	-3.86	-31.61	70.13	-46.95	0.74	0.81
100° from the strike	5.05	-11.21	4.35	7.00	-11.19	0.71	0.83
120° from the strike	4.96	-10.84	2.80	9.28	-12.25	0.70	0.88
140° from the strike	4.47	-2.65	-36.85	78.42	-51.24	0.71	0.89
160° from the strike	4.43	-3.17	-34.62	74.87	-49.45	0.68	0.90
Two recorded components	4.58	-3.54	-32.60	71.27	-47.33	0.72	0.85
Median D and median IMs	4.50	-1.48	-42.09	86.97	-55.86	0.73	0.85
Max D and median IMs	5.63	-14.73	25.03	-27.94	9.42	0.78	0.75

Table 2. The coefficients for the vector (PGA, PGV) model developed based on different displacement data.

Sliding displacement used in the regression	a_1	a_2	a_3	a_4	a_5	a_6	a_7
0° from the strike	-1.08	-4.18	-28.93	64.06	-43.10	-0.56	1.45
20° from the strike	-1.19	-2.05	-38.94	81.15	-52.46	-0.55	1.45
40° from the strike	-1.17	-2.68	-35.10	73.98	-48.35	-0.54	1.46
60° from the strike	-1.05	-3.34	-32.07	68.63	-45.28	-0.52	1.44
80° from the strike	-1.06	-2.91	-35.19	75.32	-49.57	-0.52	1.44
100° from the strike	-0.77	-10.19	0.25	13.11	-14.33	-0.57	1.46
120° from the strike	-0.80	-9.62	-2.12	16.66	-16.08	-0.57	1.45
140° from the strike	-1.24	-2.14	-38.37	79.90	-51.73	-0.56	1.47
160° from the strike	-1.18	-2.89	-34.93	74.19	-48.68	-0.56	1.46
Two recorded components	-1.07	-3.35	-32.58	70.33	-46.61	-0.53	1.44
Median D and median IMs	-1.22	-1.31	-41.84	85.38	-54.67	-0.54	1.45
Max D and median IMs	-0.22	-14.18	23.52	-26.57	9.03	-0.49	1.46

5 ORIENTATION-INDEPENDENT PREDICTIVE RELATIONSHIPS OF SLIDING DISPLACEMENT

As noted previously, the ground motion IMs used in developing the predictive relationships of sliding displacement generally are those from a set of time histories, while the definition from GMPEs combines the directionally varying IMs into a single numerical value. An orientation-independent estimation of sliding displacement is needed to ensure the consistency between the derivation of the ground motion IMs and its application in the prediction of sliding displacement of slopes. The maximum and median values of the displacement are used to represent the orientation-independent displacement. This is given as:

$$(\ln D)_{RotD100} = f(k_y, \mathrm{IMs}_{RotD50}) \quad [5]$$

$$(\ln D)_{RotD50} = f(k_y, \mathrm{IMs}_{RotD50}) \quad [6]$$

where $(\ln D)_{RotD100}$ is the 100th percentiles of the sliding displacement over all orientations (maximum sliding displacement); $(\ln D)_{RotD50}$ is the 50th percentiles of the sliding displacement over all orientations (median sliding displacement); IMs_{RotD50} is the 50th percentiles of the ground motion parameters over all orientations (median IMs), which is the definition of IMs in the latest NGA-West2 GMPEs. The regression analyses are made by using Eqs. [3] and [4]. The coefficients for the two predictive relationships are given in Tables 1 and 2.

Figure 6 shows the results of the predicted median sliding displacement of these models. Also shown are the results from the model developed by displacements and ground motion IMs of the recorded orthogonal ground motion components (M_w = 7, R_{jb} = 6 km, PGA = 0.33 g, PGV = 30 cm/s). It can been seen that the predicted displacement is consistent between the relationship developed by the median displacement and median IMs and by the displacement of the two recorded components. Thus, the commonly developed predictive relationships are essentially for the median displacement of ground motion through all horizontal orientations. However, the

predicted displacement from the relationship developed for the maximum displacement in all orientations is significantly larger than that from the former two relationships. These observations indicate that for the given ground motion IMs from GMPEs, the sliding displacement predicted from the traditional predictive relationships that are developed by displacements from particular ground motion time histories may be underestimated. Figure 7 shows the variation of standard deviation of the displacement residuals with k_y/PGA for different predictive relationships. Observe that the standard deviation decreases when using the orientation-independent displacements and IMs_{RotD50} compared to that from the traditional relationships, particularly when using the median displacement in the model development. This could be another benefit of the orientation-independent relationship of sliding displacement of slopes.

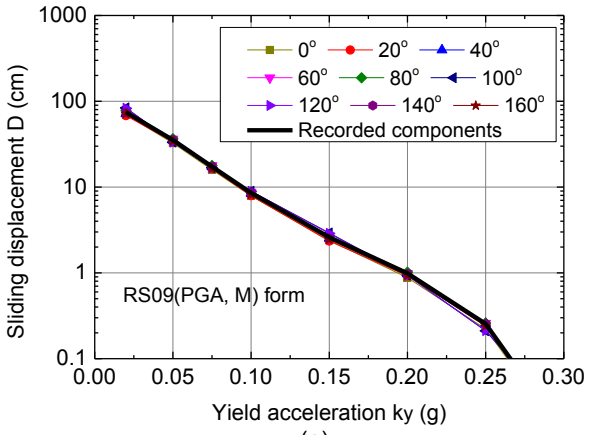

(a)

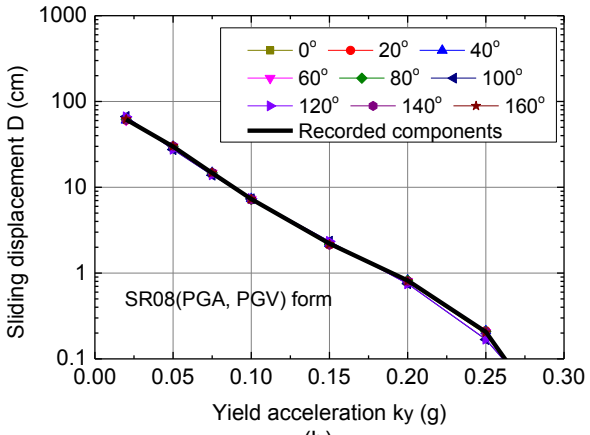

(b)

Figure 4. Predicted median sliding displacement of various models that developed based on the computed displacement data of ground motions in various orientations (M_w = 7, R_{jb} = 6 km, PGA = 0.33 g, PGV = 30 cm/s): (a) The RS09(PGA, M) form; (b) The SR08(PGA, PGV) form.

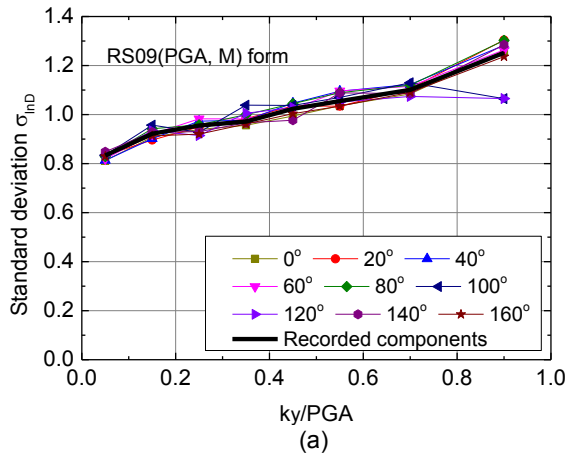

(a)

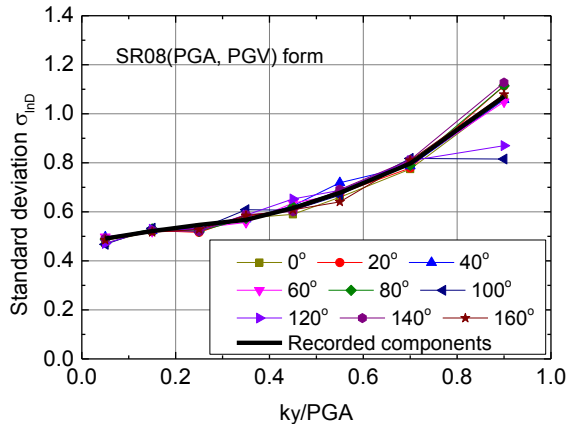

(b)

Figure 5. Standard deviation of various models that developed based on the computed displacement data of ground motions in various orientations: (a) The RS09(PGA, M) form; (b) The SR08(PGA, PGV) form

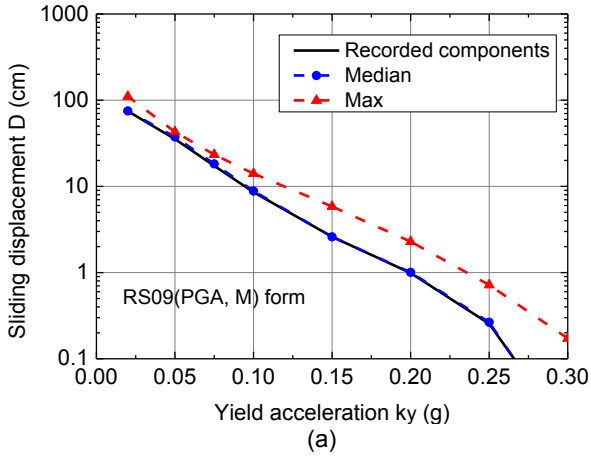

(a)

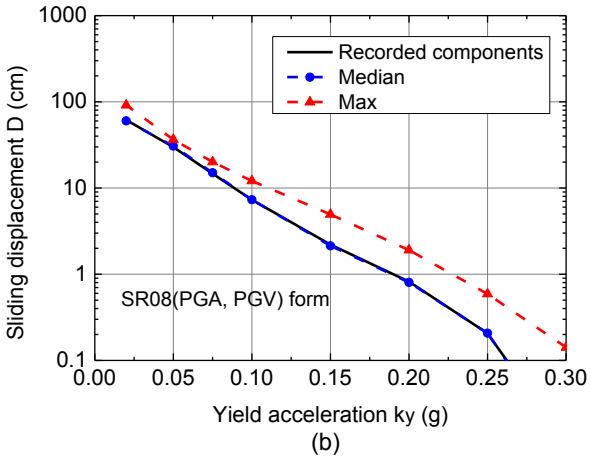

(b)

Figure 6. Predicted median sliding displacement of models that developed using the displacements of the recorded ground motion components as a function of IMs in the time histories, using the median and maximum displacements as a function of the median IMs, respectively (M_w = 7, R_{jb} = 6 km, PGA = 0.33 g, PGV = 30 cm/s): (a) The RS09(PGA, M) form; (b) The SR08(PGA, PGV) form.

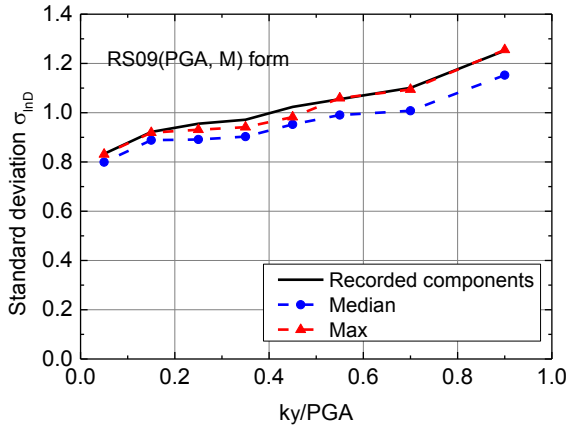

(a)

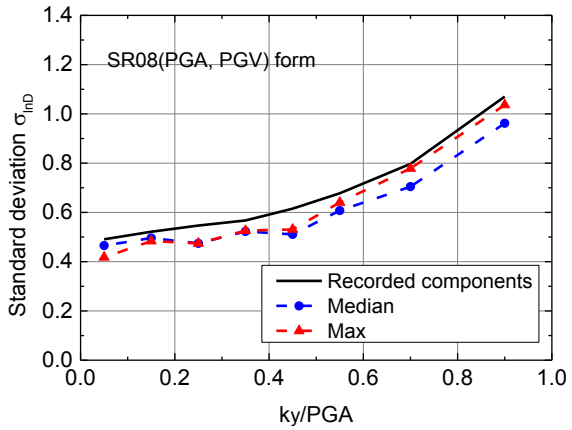

(b)

Figure 7. Standard deviation of models that developed using the computed displacements of the recorded orthogonal ground motion components as a function of IMs in the time histories, using the median and maximum displacements in all orientations as a function of the median IMs in all orientations, respectively: (a) The RS09(PGA, M) form; (b) The SR08(PGA, PGV) form.

6 CONCLUSIONS

A set of ground motion records from the NGA-West2 database are selected and the rigid sliding displacement are computed for each ground motion record by rotating the horizontal components through all angles. The distribution of sliding displacements in various orientations are examined. The observations indicate that the sliding displacement can be dependent on the orientation of ground motions. The orientation in which the maximum sliding displacement occurred is also examined. A pronounced polarity of the sliding displacement to the fault-normal direction is observed for ground motions with R_{rup} < 5 km, while the maximum direction orientation is almost uniformly distributed for ground motions with R_{rup} > 5 km, which is consistent to the observations in ground motion directionality.

Predictive relationships of the sliding displacement are developed by using the computed displacement data of ground motions in various orientations. The predictive relationship is independent of the orientations in which the displacement data is used. Two orientation-independent estimation of sliding displacement are developed by using the median and maximum displacements as a function of the median IMs in all orientations. The predicted displacement of the relationship developed by the median displacement and median IMs is consistent with that from the relationship developed using the displacements of two recorded ground motion components as a function of IMs in the time histories. The predicted displacement from the relationship developed by the maximum displacement and median IMs is significantly larger than that from the former two relationships. The standard deviation decreases for the relationship that developed using the orientation-independent displacements and the median IMs used in GMPEs compared to the traditional models.

The developed orientation-independent estimations of the earthquake-induced sliding displacement of slopes use the directionally-dependent ground motion IMs as predictors. These ground motion parameters are consistent with those used in the latest ground motion prediction equations of NGA-West2 program of PEER.

ACKNOWLEDGEMENTS

This research has been supported by the National Natural Science Foundation of China (Grant No. 41602280 and 41630638), National Key Basic Research Program of China (Grant No. 2015CB057901), National Key Research and Development Program of China (Grant No. 2016YFC0800205), China Postdoctoral Science Foundation (Grant No. 2016M601708), the Fundamental Research Funds for the Central Universities in China

(Grant No. 2016B01114). These supports are gratefully acknowledged.

REFERENCES

Ambraseys, N.N., Menu JM. 1988. Earthquake-induced ground displacements, *Earthquake Engineering & Structural Dynamics*, 16(7): 985-1006.

Ancheta, T.D., Bozorgnia, Y., Darragh, R., Silva, W.J., Chiou, B., Stewart, J.P., Boore, D.M., Graves, R., Abrahamson, N.A., Campbell, K.W., Idriss, I.M., Youngs, R.R., Atkinson, G.M. 2012. PEER NGA-West2 database: A database of ground motions recorded in shallow crustal earthquakes in active tectonic regions, *In 15th Word conference on earthquake engineering, Lisbon, Portugal*.

Boore, D.M. 2010. Orientation-independent, nongeometric-mean measures of seismic intensity from two horizontal components of motion, *Bulletin of the Seismological Society of America*, 100(4): 1830-1835.

Boore, D.M., Stewart, J.P., Seyhan, E., Atkinson, G.M. 2014. NGA-West2 equations for predicting PGA, PGV, and 5% damped PSA for shallow crustal earthquake, *Earthquake Spectra* 30(3), 1057-1085.

Bray, J.D., Travasarou, T. 2007. Simplified procedure for estimating earthquake-induced deviatoric slope displacements, Journal *of Geotechnical and Geoenvironmental Engineering*, ASCE, 133(4): 381-392.

Howard, J.K. Tracy, C.A. Burns, R.G. 2005. Comparing observed and predicted directivity in near-source ground motion, *Earthquake Spectra,* 21(4): 1063-1092.

Hsieh, S.Y., Lee, C.T. 2011. Empirical estimation of the Newmark displacement from the Arias intensity and critical acceleration, *Engineering Geology* 122(1-2): 34-42.

Huang YN, Wittaker AS, Luco N. 2008. Maximum spectral demands in the near-fault region, *Earthquake Spectra*, 24(1): 319-341.

Huang YN, Wittaker AS, Luco N. 2009. Orientation of maximum spectral demand in the near-fault region, *Earthquake Spectra*, 25(3): 707-717.

Jibson, R.W. 2007. Regression models for estimating coseismic landslide displacement, *Engineering Geology,* 91(2-4): 209-218.

Lee, J., Green, R.A. 2015. Empirical predictive relationship for seismic lateral displacement of slopes, *Géotechnique,* 65(5): 374-390.

Makdisi, F.I., Seed, H.B. 1978. Simplified procedure for estimation dam and embankment earthquake induced deformations, *Journal of the Geotechnical Engineering Division*, ASCE, 104(GT7): 849-868.

Newmark, N.M. 1965. Effects of earthquakes on dams and embankments, Géotechnique, 15(2), 139-160.

Rathje, E.M., Antonakos, G. 2011. A unified model for predicting earthquake-induced sliding displacements of rigid and flexible slopes, *Engineering Geology,* 122(1-2): 51-60.

Rathje, E.M., Saygili, G. 2009. Probabilistic assessment of earthquake-induced sliding displacements of natural slopes, *Bulletin of the New Zealand Society of Earthquake Engineering,* 42(1): 18-27.

Saygili, G., Rathje, E.M. 2008. Empirical predictive models for earthquake-induced sliding displacements of slopes, *Journal of Geotechnical and Geoenvironmental Engineering*, ASCE, 134(6): 790-803.

Shahi, S.K., Baker, J.W. 2014. NGA-West2 models for ground-motion directionality, *Earthquake Spectra,* 30(3): 1285-1300.

Song, J., Gao, G.Y., Rodriguez-Marek, A., Rathje, E.M. 2016. Seismic assessment of the rigid sliding displacements caused by pulse motions, *Soil Dynamics & Earthquake Engineering,* 82: 1-10.

Song, J., Rodriguez-Marek, A. 2015. Sliding displacement of flexible earth slopes subject to near-fault ground motions, *Journal of Geotechnical and Geoenvironmental Engineering*, ASCE, 141(3): 04014110.

Watson-Lamprey, J.A., Boore, D.M. 2007. Beyond SaGMRotI: Conversion to SaArb, SaSN, and SaMaxRot, *Bulletin of the Seismological Society of America,* 97(5): 1511-1524.